

# 2

---

## The State of the Art of Research Concerning Vibroacoustic Diagnosis of Machine Tools

Monitoring and diagnosis of machine tools and technological equipment on the basis of vibration and noise analysis has greatly expanded in the last twenty years. Although a relatively young field of research, this domain is marked by important theoretical and experimental findings that are selectively presented in this chapter.

### 2.1 DIAGNOSIS OF ROLLING BEARINGS

Bearings are a major source of vibration and noise in machine tool manufacturing. Their vibration and noise level correlate with their functioning state, indicating the presence and eventually the evolution of some damage. Thus, interventions must be made in order to avoid serious damage.

For bearings in a nonmounted state a sum of characteristic frequencies is highlighted: the rotation frequency of the bearing cage  $f_c$ , the frequency of the ball running on the internal inner  $f_I$ , and the ball rotation frequency  $f_b$ . These frequencies depend on the rotation frequency of the spindle  $f_n$ . [Table 2.1](#) presents the values of these frequencies for several types and sizes of bearings. It can be observed that the  $f_c < f_n < f_e < f_e < f_I$  relation always exists. Maintaining the relation

**TABLE 2.1** Characteristic Frequencies for Bearings in Nonmounted State

Frequency (Hz)	Bearing 6206	Bearing 6209	Bearing 7309
$f_c$	$0.391 f_n$	$0.402 f_n$	$0.410 f_n$
$f_e$	$3.132 f_n$	$3.621 f_n$	$4.506 f_n$
$f_i$	$4.868 f_n$	$5.379 f_n$	$6.497 f_n$
$f_b$	$2.191 f_n$	$2.460 f_n$	$4.022 f_n$

between the characteristic frequencies shows that the shape and sizes of the rolling bodies influence these frequencies only in small measure [46].

The vibrations and noise produced by the bearings in a mounted state manifest themselves not only by direct effects (acoustic radiation, vibration), but also indirectly (on the level of other elements, on the route source-receiver). The main causes that lead to an increase of the noise and vibrations on the mounted bearings are:

Changing the position of the rolling bodies in the charged (respectively, uncharged) zone of the bearing, taking into consideration the elastic contact deformations and the working play

The nonuniform movement of the rolling bodies, which leads to friction and collisions of the rolling bodies with the rings and the cage

The contact that appears on the rolling movement on the surfaces with dimensional, shape, and position deviations (deviations of diameter, axial or radial runout of the rolling paths, eccentricity, ovalization, polygonality, waviness)

Passing of the rolling bodies over the impurities from the contact surfaces or over damages or local deterioration (pitting or peeling, abrasive wear, prints)

Table 2.2 synthetically presents relations concerning the position of the peak in the frequency spectrum for these damages; the data have been considered for the bearing with turning internal ring ( $f_i = f_n = n/60$ ) and fixed external ring. The notations represent:  $f_{ci}$ , turning frequency of the cage function of the internal ring;  $f_{ce}$ , turning frequency of the cage function of the fixed external ring; and  $f_{be}$ , the turning frequency of the rolling bodies function of the fixed external ring.

**TABLE 2.2** Relations Concerning Position of the Peak in the Frequency Spectrum for Damages at Mounted Bearings

Element	Deviation	Position of peak in spectrum, Hz (linear effects)	Position of peak in spectrum, Hz (nonlinear effects)
Internal ring	Radial runout	$f_i$	—
	Waviness	$mzf_{ci} \pm pf_i m z$	$mf_{ci} \pm f_{ce}$
	Singular damage (pitting)	$f_{ci} \pm pf_i$	
External ring	Waviness/singular damage	$mzf_{ce}$	$(m \pm 1)f_{ce}$
Rolling body	Diameter variation	$mf_{ce}$	—
	Waviness	$2mf_{be} \pm pf_{ce}$	—
	Singular damage	$2mf_{be} \pm pf_{ce}$	—

The frequency that corresponds to the succession in-out of the rolling bodies from the singular damages can be estimated with the equation:

$$f_t = \pi D_m n \left[ 1 - \left( \frac{D_b}{D_m} \cos \alpha_B \right)^2 \right] / (2b) \quad (2b)$$

where  $b$  is the damage length on the circumference of the rolling path.

Monitoring of the vibration level can indicate nearly all types of mechanical faults of the dynamical equipment. An increased vibration level signals imbalance, nonalignment, general wear, or play between subassemblies; a high shock impulse level signals a nonalignment, an incorrect lubrication, or the existence of an overload on the bearing.

A rapid and efficient method of monitoring the functional state of the bearings, named the shock impulses method, has been patented by the Swedish company SPM (Shock Pulse Meter). The principle and mathematical apparatus of the method are presented in great detail in this paper. The level of shock impulses of a bearing depends on the size of the bearing, the rotation speed, and the working conditions.

The SPM equipment can indicate the limit values for good, reduced, and unsatisfactory functioning conditions for any kind of bearing. [Figure 2.1](#) presents a monitoring system for simultaneous supervision of 16 measuring points. The scavenged frequency domain is between 10 and

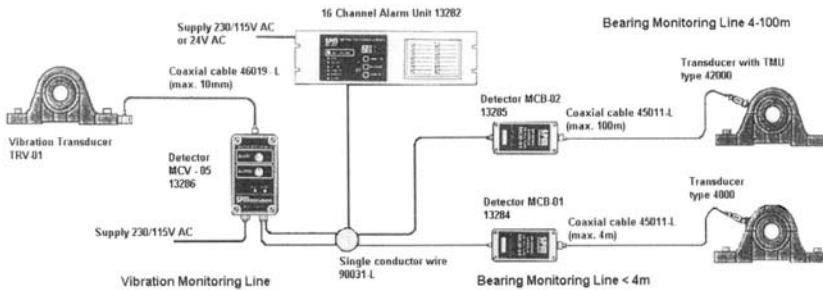


**FIGURE 2.1** Monitoring system.

10,000 Hz, corresponding to the ISO 2372 recommendations (equivalent to BS4675 and VDI2056). The measurement is made on (a) channel ALERT, which is mainly used to monitor significant increase of the vibration level due to wear, a channel with a discrete adjustable level from 25 to 75 dB<sub>SV</sub>; and (b) channel ALARM, which is used to warn and to stop voltage feeding of the monitored machine. [Figure 2.2](#) illustrates the estimation graphics of the functioning state of the bearings.

Frequency analysis of the vibration signal is the most efficient diagnostic method for bearings. During the first investigation, the vibration level in the large band (third octave) or narrow band (10%, 3%, 1%) can be analyzed. This way the power of the signal can be appreciated, and the frequency peaks can be located in order to diagnose them (see [Table 2.2](#)). This process is complicated by the fact that the frequency peaks do not manifest themselves in a uniform way on the whole spectrum: at low frequencies they can be masked by white noise, and at high frequencies the danger of resonance appears. It must be noted that the position in the frequency spectrum presented previously depends on the bearing turn, because the position in the frequency spectrum previously presented is independent of turn ([Figure 2.3](#)).

Because of the presence in the spectrum of numerous harmonics that disturb the signal interpretation (some of them hide significant frequencies), Cepstrum analysis is recommended in bearings diagnosis [19]. This way it is possible to detect the periodicity in the spectrum (families of harmonics and lateral bands), the analysis also being insensitive to perturbations that appear on signal transmission. Detection by Cepstrum analysis of damage in a large-sized bearing ([Figure 2.4](#)) highlights the presence in the spectrum of the frequency of the pass of the

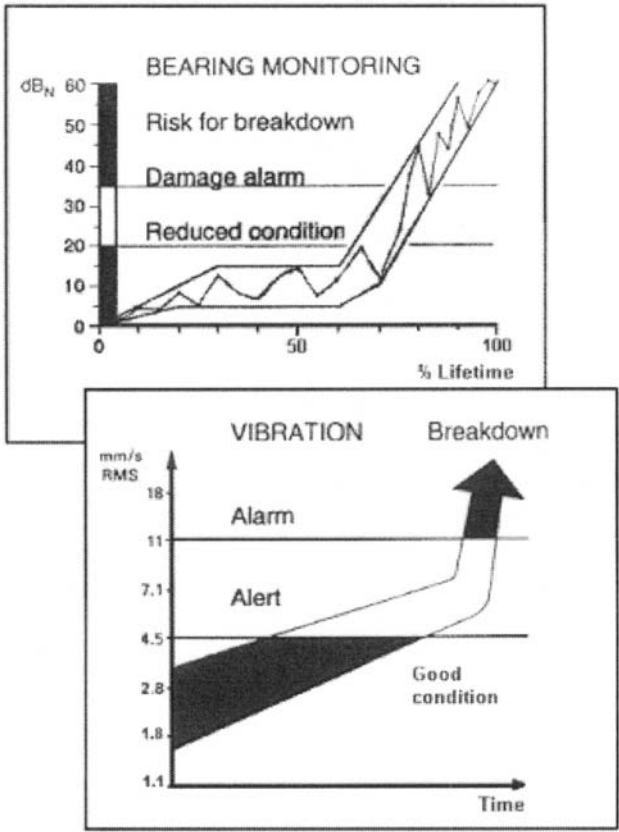


**FIGURE 2.2** Estimation of the functioning state of the bearings.

rolling bodies over a pit from the external ring (FTBO), and also its first harmonics.

Frequency analysis has given birth to a spectacular method of investigation of the vibration signal, a method of comparing the spectra. The Danish company, Brüel & Kjær, launched the method and made it operational. The differences between the measured current spectrum and the spectrum templates come from the boarding of the reference signal. If the current spectrum surpasses the tolerance template, a warning signal is emitted and, if the limit template is surpassed, the emitted signal is one of damage and in parallel the machine is stopped. The method

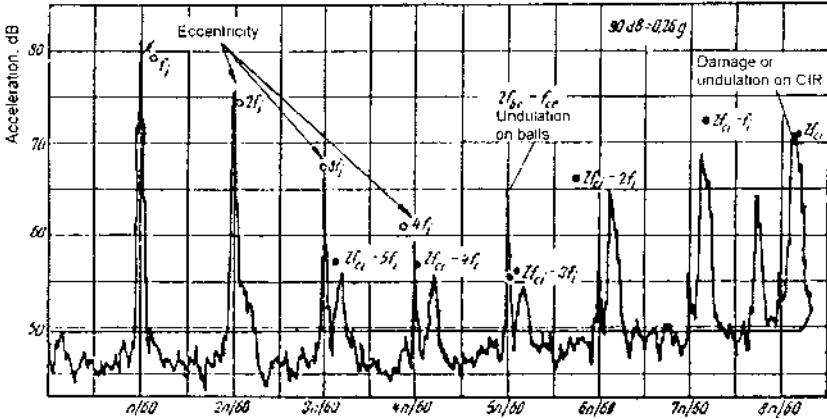


FIGURE 2.3 Analysis in frequency—spectrum.

can be completed by an analysis of the tendency of the frequencies that bypass the tolerance templates, the analysis that approximates the time until the final damage. Figure 2.5 illustrates the use of this method as a diagnostic of large-sized bearings: (a) comparing the current spectrum with the tolerance template; (b) graphic highlighting of the spectrum

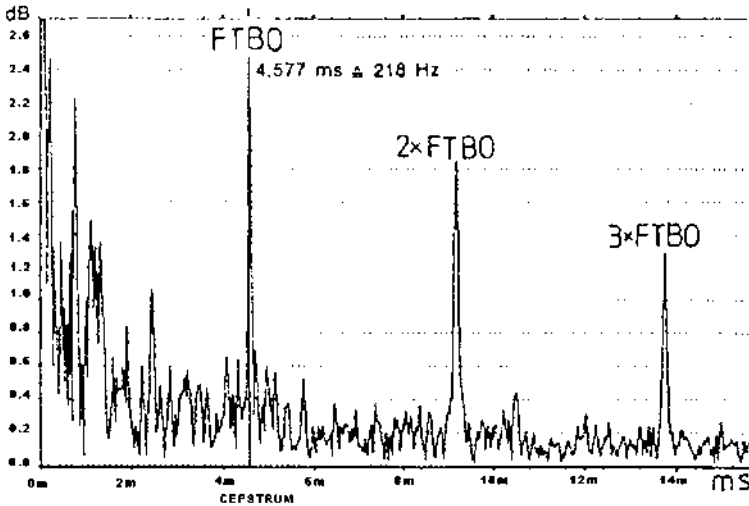
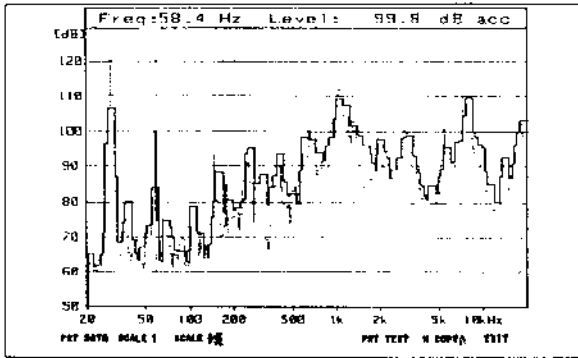
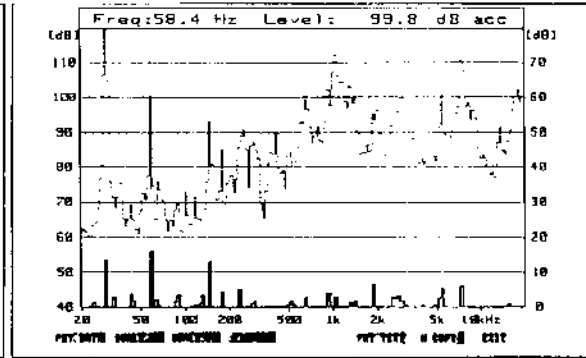


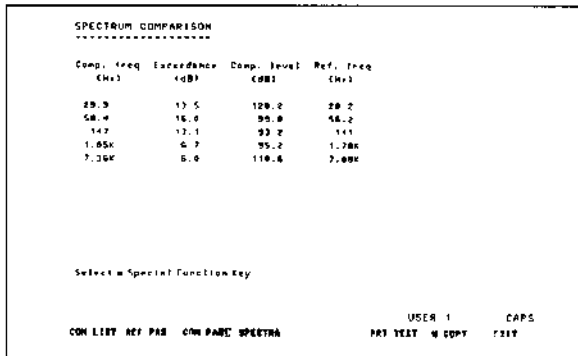
FIGURE 2.4 Detection of damage on bearings by Cepstrum analysis.



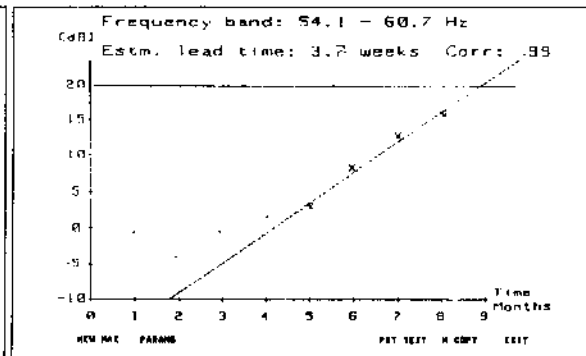
a)



b)



c)



d)

**FIGURE 2.5** The method of spectrum comparison: (a) comparing the current spectrum with the tolerance template; (b) graphic highlighting of the spectrum displacements on narrow frequency bands; (c) selection of the alarming bypasses of over 6 dB; (d) drawing the tendency graphic for one of the selected frequencies.

displacements on narrow frequency bands; (c) selection of the alarming bypasses of over 6 dB; and (d) drawing the tendency graphic for one of the selected frequencies.

Another powerful method of frequency analysis, useful in diagnosis of bearings and also of gears and hydraulic elements is frequency analysis of the evolute of an intermediate signal from the time domain. The sure advantages of this method consist of highlighting the periodicity of the peaks corresponding to the damages from the bearing, their separation from the signals with close frequencies, or from the frequencies excited by resonance. Dr. D. Pupaza used this method with good results in the diagnosis of roller bearings, in the frame of a specialization at the University of Leicester (United Kingdom). He applied the method to diagnose the bearings of the main shaft of a NC milling machine (Figure 2.6). The tests were made at idle running (2400 rpm) to minimize slippage and contact angle variation. The results obtained at the introduction of damage on the internal ring confirmed the increase in amplitude at the frequency estimated by calculus [126].

Acoustic signals are used for the diagnosis of bearings in the non-mounted state. Because of the reduced noise general level, the diagnosis of the bearings mounted in an assembly that contains other sources presents serious difficulties. The bearing under research is placed on a stand having very quiet characteristics, located in an anechoic chamber having inferior minimum frequency under 250 Hz. The placement of the free field microphone is indicated in Figure 2.7.

In his doctoral thesis, D. Radauceanu [128] analyzed the problem of noise dependence of the radial bearings upon the manufacturing and functioning conditions, and highlighted some interesting general aspects:

A correlation exists between the noise and vibration levels of the same bearing under the same measuring conditions, and is evident in the frequency analysis of large band and less perceptible to frequency analysis of narrow band.

The shape deviations of the rings and rolling bodies (microgeometry, waviness, roughness) negatively influence the noise and vibration levels.

Ball bearings are quieter than roller bearings (5 to 10dB).

A watertight bearing, lubricated with low viscosity grease has a noise level smaller than an open one (3 to 4dB).

Mounting a roller in a soft gearing box (i.e., silicone rubber) or in a fixed position, reduces the noise with 6–10dB.



Vibration source	The excitation frequency at 2040 rpm [Hz]
Main spindle (shaft)	34
Rolling element <sup>RI</sup>	473
Interior ring <sup>RI</sup>	348
Exterior ring <sup>RI</sup>	264
Rolling element <sup>RS</sup>	465
Interior ring <sup>RS</sup>	329
Exterior ring <sup>RS</sup>	249

RI = Lower bearing  
RS = Upper bearing

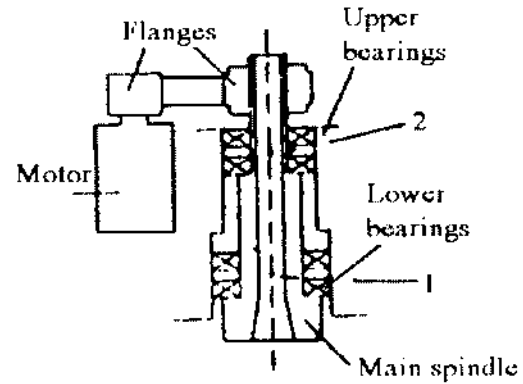


**FIGURE 2.6** Diagnosis of main spindle bearings of a milling machine using frequency analysis of the evolute of an intermediate signal.

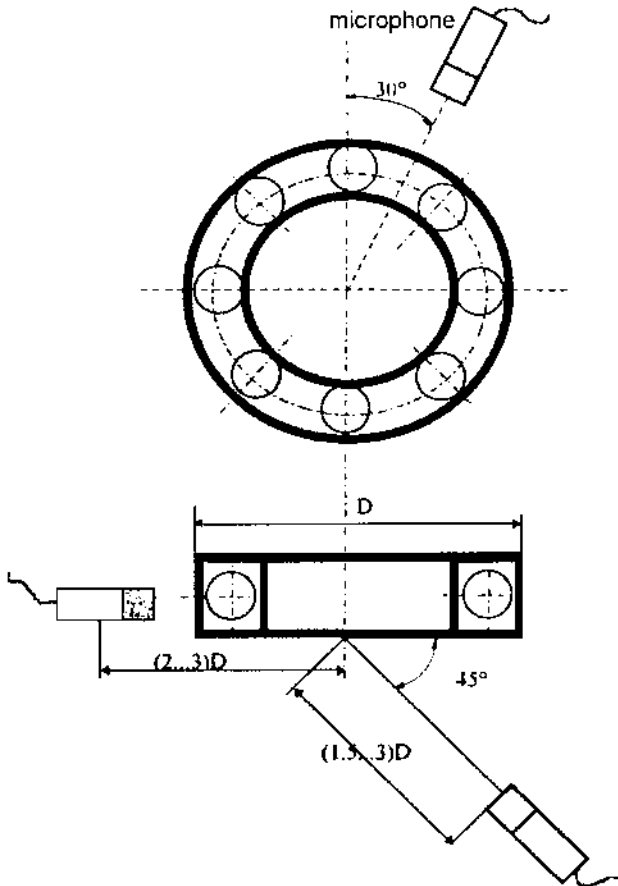


**FIGURE 2.7** Diagnosis of main spindle bearings using spectrum comparison.

Load influences the noise level of the bearings very little, but the rpm considerably influences it (the acoustic pressure is approximately proportional to the square of the turn).

No relevant differences of the noise level were observed between lubrication with low viscosity level and oil lubrication [128].

## 2.2 DIAGNOSIS OF SLIPPING BEARINGS

Slipping bearings are less frequently used in machine tool manufacturing. However, they may determine supplementary perturbations in the

functioning of kinematic chains, usually with minor effects. The axle bearing in this case constitutes the main cause of the noise and vibrations. If radial plays in this kinematic couple also exist, they generate in spectrum peaks of the frequency of the axle  $f_o$  and of the subharmonics of this frequency ( $f_o/2, f_o/3$ ).

If the following phenomena are present: insufficient feeding with lubricant of the bearing, overloading of the axle (forces and moments), changing the rotation direction of the axle, and instability of the lubricant film at high rpm, then these lead to a thinner lubricant film and the occurrence of the “fiddlestick” phenomenon, which produces a noise with spectrum peaks at the rotation frequency of the axle  $f_o$  and at the harmonics of this frequency ( $2f_o, 3f_o, \dots$ ).

The diagnosis of these bearing types is chiefly carried out by supervising the noise and the acoustic emission. The acoustic signal is detected, amplified, and filtrated by filter pass-up and then analyzed in the time domain. The averaging of the signal in amplitude (RMS) and the recording of the impulses that pass over a limit value, adjustable, of the amplitude are executed [39].

The change from the hydrodynamic friction to the mixed frequency is indicated by the occurrence of some peaks in the domain of the high frequencies, emitted as a result of going beyond the carrying capacity of the bearing. The frequency analysis puts in evidence the phenomenon through a dominant in front of the rotation frequency of the shaft.

The spectral density of the impulse function can correlate very well with the functioning state of the bearing, as highlighted in Figure 2.8.

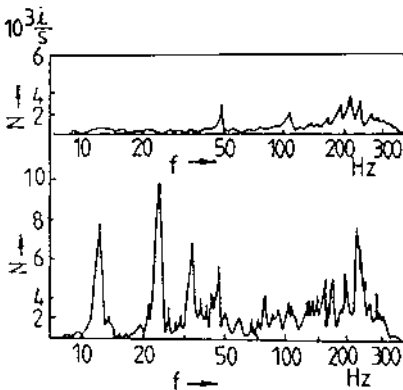


**FIGURE 2.8** Spectrum of the impulse density for a hydrodynamic bearing.

The upper part of the figure presents the spectrum of the impulse density for the hydrodynamic bearing in perfect condition, and the lower part of the figure presents the spectrum of the same bearing, this time damaged.

In order to reduce the noise and vibrations generated by the slipping bearings, some measures can be taken:

Choosing an eccentricity relatively bigger than an admissible value  $\varepsilon = 0.2-0.3$ , ensuring the stability of the axle

Ensuring a correct lubrication

Modifying the shaft rpm in order to avoid functioning at the critical rpm or double of this critical rpm

Equilibrating the shaft in bearings, by the mean of the marks that are mounted on the axle

## **2.3 DIAGNOSIS OF GEAR WHEEL TRANSMISSIONS**

The gears constitute one of the most important sources of noise and vibration in the machine tool structure. The gears' vibroacoustic behavior becomes more defective as the transmitted power and the rpm increase, and with the decrease in the size of gears. The parameters that determine the vibroacoustic behavior of the gears can be grouped depending upon their nature:

Constructive parameters (module, inclination angle, covering extent, number of teeth, material, etc.)

Technological parameters (the class of precision, execution errors, roughness, etc.)

Functional parameters (rotation speed, load, moment, existence of lubricant)

Table 2.3 synthetically presents the influence of the constructive parameters on the vibroacoustic level of the gear wheel transmissions. It should be noted that the main factor influencing the vibroacoustic level of the gear wheel transmissions is the teeth inclination followed by the stiffness of the gear wheel material. The gear's behavior on the dynamic regime is especially influenced by the parameters belonging to the two groups. The execution and mounting errors determine supplemental relative movements of the wheels, which superimpose those determined by the variable stiffness of the gear. The most important increase of the noise level (up to 20 dB) is determined by the shape errors

**TABLE 2.3** Influence of Constructive Parameters on Vibroacoustic Level of Gear Wheel Transmissions

Analyzed parameter	Analyzed values domain	Influence of parameter value increase on noise level (dB)
Tooth inclination	0–40	↓20
Material stiffness	—	↑12
Tooth flank	0–0.02 mm	↓6
Covering extent	1–2.2	↓3
Module	1–12 mm	↑2
Number of teeth	$z-2z$	↑3
Specific deviation of profile	0.092–0.883	↓1
Width of tooth	—	Low effect
Tooth bulging, stiffness, mass of frame box	—	To large direction errors of tooth

of the profile. They imply increased frequencies that can coincide with the natural frequency of the transmission. The decrease of the working surfaces' roughness (by shaving, grinding) leads to a decrease of 3 to 4 dB of the noise level. If the relative error of the base step is positive, the gearing begins and ends beyond the theoretical gearing line; thus, the entrance and exit of the tooth from the gearing is made in shock conditions. The rotation error cumulates the effect of deformations and the errors of the teeth, providing complete indications on the mechanism of the excitation.

Concerning the exploitation parameters, experimental research has shown that the noise and vibration levels increase at the same time as the load and angular speed. Doubling the loading moment has the effect of increasing the noise level by 3 to 4 dB. On the other hand, the doubling of the rpm produces an increase of 6 to 7 dB, at the same loading. The influence of the oil viscosity on the vibroacoustic behavior of gears is negligible [106].

The analysis in the frequency domain is the most adequate technique for processing the vibroacoustic signal coming from the gearing, because the modifications of some spectral components correlated to the evolutionary damages that do not sensibly affect the global vibration level are detectable in the frequency spectrum, and the modifications of the spectrum provide important information concerning the causes

of the damage. Usually, the frequency spectrum of the noise and vibration from gearing presents peaks at: (a) the gearing frequency and its harmonics, (b) secondary components, (c) lateral bands, and (d) low harmonics of the rotary frequency.

(a) The harmonics of the gearing frequency: the gearing frequency can be calculated as the multiplication between the rotation frequency of the shaft ( $f = n/60$ ) and the number of teeth of the wheel  $z$ , so  $f_a = f * z$ . The spectrum peaks corresponding to the gearing frequency and its harmonics are caused by the shocks, which arise in gearing because of the deviations from the ideal profile (Fig. 2.9). These deviations occur either during manufacturing or by the nonuniform wear of the flanks, which is larger on both sides of the rolling circle. The wear presence is more evident to the superior harmonics.

(b) The secondary components (accidental) occur in the same conditions as the gearing frequency and its harmonics, but correspond to a different number of teeth, and these secondary components are due to kinematic errors of the generating kinematic chains of the gear-tooth cutting machine. The most important of these errors is the gear-tooth cutting error on the rotation of the gear-tooth cutting table. If the wheel has a number of  $N_o$  teeth on the functioning of the gear wheel on the table activated by it, a frequency will appear corresponding to  $N_o$ , as the harmonic integer multiple of the rotation frequency. This component is easily recognized because of its property of being independent by the increase of the load.

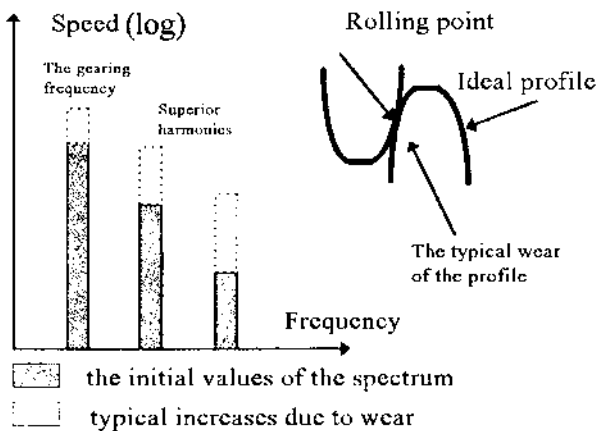


**FIGURE 2.9** Gearing frequency harmonics.

(c) The lateral bands around the gearing frequency and its harmonics can be explained by the amplitude modulation or the nonuniform vibration frequency of the gearing, caused by some local damage. For example, the radial runout of the gear or the eccentricity of the gear wheels' sustaining shafts make the division circles of the two gearing wheels not remain tangent during the whole gearing time. Because of this radial runout, the low frequency corresponding to the rotational movement with  $f_i$  frequency superimposes a relatively high frequency vibration corresponding to the gearing process  $f_a$ , resulting in a vibration modulated in amplitude. In the limit case of a 100% modulation, the  $f_i$  component disappears, and the lateral frequencies characteristic to modulation remain:  $f_{1\text{ inf}} = f_a + f_1$  and  $f_{1\text{ sup}} = f_a - f_1$ . Because the modulation process is distorted by manufacturing errors and 100% modulation is not realized, peaks arise in the spectrum for frequencies  $f_{j\text{ inf}} = f_a - j * f_1$  and  $f_{j\text{ sup}} = f_a + j * f_1$ , with  $j = 2, 3, 4, \dots$ . Also, every fluctuation in the tooth load will have the tendency to generate a variation of the vibration amplitude, so an amplitude modulation appears. At the same time, those fluctuations also determine fluctuations of angular speed, so a frequency modulation appears. The two modulations determine an increase of the lateral bands of frequency amplitude, their distance in the spectrum being equal to the modulation frequency. This contains important information on the source of the modulation effect. Each modulation with a pure frequency tends to give a family of lateral bands, and in the case where the modulation is not pronounced, this can be represented by two or three groups of lateral bands. Under these conditions, an additional effect is to increase the number of lateral bands.

(d) The low harmonics of the rotation frequency correspond to the cumulated impulses that repeat with each rotation of the wheel. The modulation in amplitude or frequency has the tendency to give symmetric signals. Any asymmetry of the signal can be interpreted as an additive signal that also gives a number of harmonics of the respective frequency.

In addition to the mentioned frequencies, other significant components may appear in the spectrum, independent of rotation, corresponding to some self-modes of vibrations for the gearing, shafts, gear box, and the like. Also, the variation function of time of the rigidity of the tooth gearing has a specific action. The parametric vibrations of the gearing are characterized in this case by the existence of many domains of instability to frequencies equal to rational fractions, multiples, or submultiples of the self-frequencies of the system. A resonance phenomenon can appear

for the same reason, when the excitation frequency  $f_e$  corresponds to one of the first subharmonics of the fundamental self-frequency  $f_i$ .

In conclusion, the frequency spectrum of the gearing transmission permits an evaluation of the mechanical state of the transmission to be made. In order to identify the sources of noise and vibration, a correlation of the frequencies corresponding to the maximums of the spectrograms with the frequencies of the possible sources from transmission is made, calculated on the basis of their constructive and functional parameters.

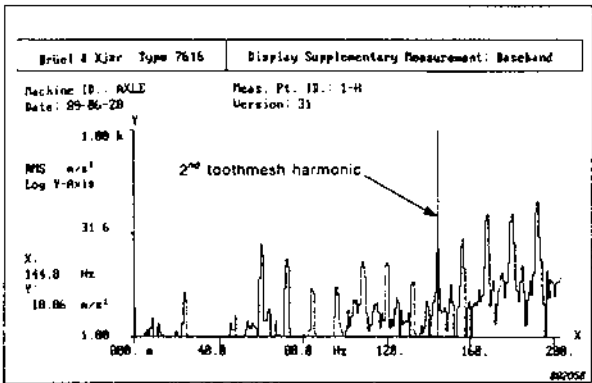
Cepstrum analysis is a powerful and useful instrument of investigation for gear transmissions. It allows detection of periodicity of the spectrum and the precise determination of the frequency of the signal modulation. In the gear diagnosis domain, the Danish company Brüel & Kjær has had notable results beginning in the 1980s. An excellent example is the diagnosis of some problems that occur in the differential mechanisms in trucks produced by Raba (Hungary) in collaboration with Brüel & Kjær.

The test consists of rolling the differential mechanism on a stand until the damage occurs, simulating diverse loading (resistant moments). The gear vibrations are permanently monitored, making it possible to stop the test at any moment in order to study the damaging mechanisms before the progress of the damage makes it impossible to recognize the source. The initiation of the damage is recognized by the increase of the characteristic frequencies and of the lateral bands around these characteristic frequencies (the Cepstrum analysis method) [14].

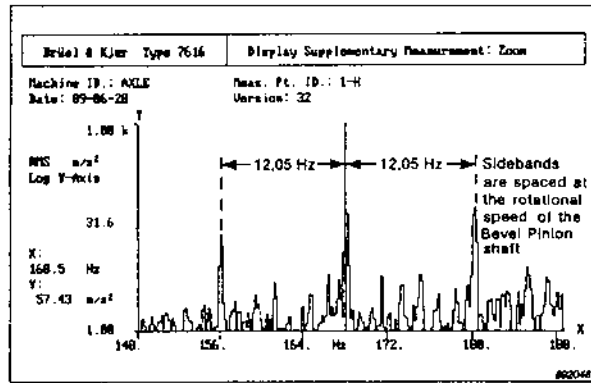
The gearing frequency is sufficiently low, so many harmonics of this frequency are included in a spectrum of 2 kHz. The monitoring of this zone has indicated the increase of the second and third harmonics' amplitude because of the debut of the pitting phenomenon to the gear teeth. As the phenomenon progresses, the lateral bands around these harmonics increase. [Figure 2.10](#) presents recordings obtained after the damage due to pitting has put gear functioning into danger. In [Figure 2.10a](#), the gearing frequency and its harmonics are evident, and a magnification in the zone of interest (the second harmonic, [Fig. 2.10b](#)) shows an excessive increase in the lateral bands, at a distance of 12.05 Hz. The point of occurrence of the lateral bands can not be exactly predicted but mathematical modeling of the damages and the perturbations introduced by these damages allows prediction.

By processing the signal by Cepstrum analysis ([Fig. 2.10c](#)), the periodicities become evident, cumulated in a single band that corresponds to the frequency of 12.05 Hz. The analysis also indicates the occurrence

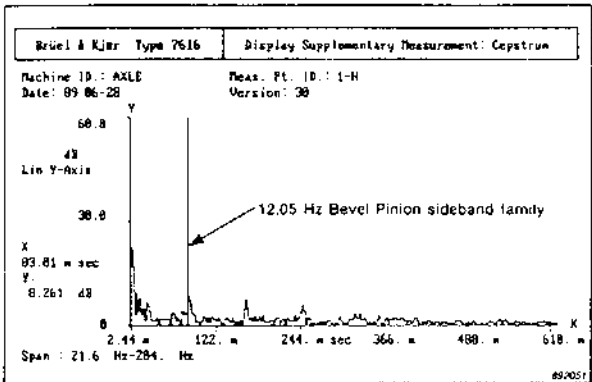




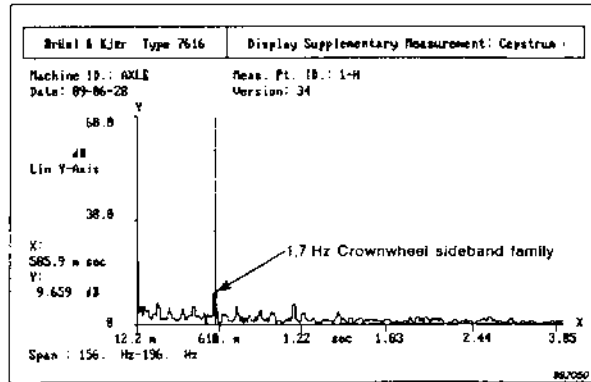
a.



b.



c.



d.

**FIGURE 2.10** Recordings obtained after damage due to pitting that puts a gear function into danger: (a) gearing frequency and its harmonics; (b) magnification of interest zone; (c) Cepstrum analysis; (d) occurrence of wear and periodicities of the lateral bands.

of wear for the gear crown, and, in this case, the periodicities of the lateral bands are grouped to 1.7 Hz (Fig. 2.10d). This highlights the fact that diagnosis of gear damage is possible by correctly processing the vibration signal, using methods from the domain of frequency analysis.

The Department of Machine Parts and Mechanisms of the Polytechnic Institute of Iasi has developed some original research on the noise and diagnosis of gearing. V. Merticaru (1971) tackled the problem of dependence of the cylindrical gear wheels on manufacturing and working conditions [106]. In his doctoral thesis (1987), B. Dragan continued this research with his contribution to noise and vibration reduction in the gearbox of machine tools. His research focused on identification of critical natural frequencies and of different kinds of damage in the gearbox of a milling machine, the kinematic scheme of which is presented in Figure 2.11 [39].

To diagnose damage, the determination of natural frequencies, modulation frequencies, and periodicities from the frequency spectrum has necessitated the building of a complex schema for analysis of the vibroacoustic signal, an analogue type schema having compression possibilities, Zoom analysis, and Cepstrum analysis (Figure 2.12).

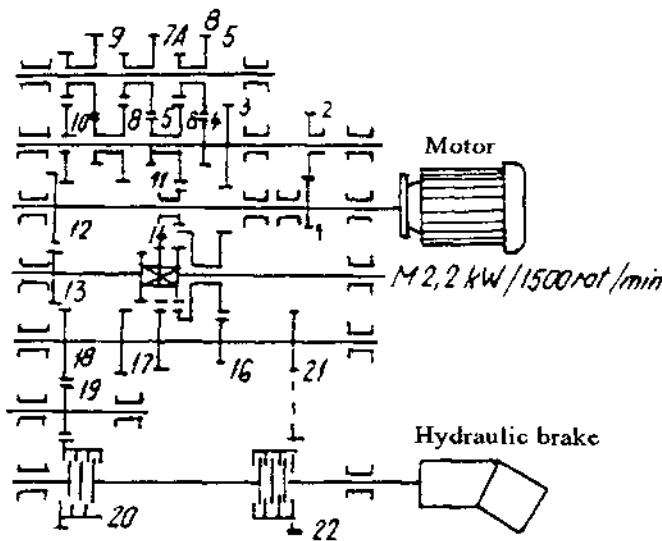


**FIGURE 2.11** Schematic of gearbox of a milling machine.

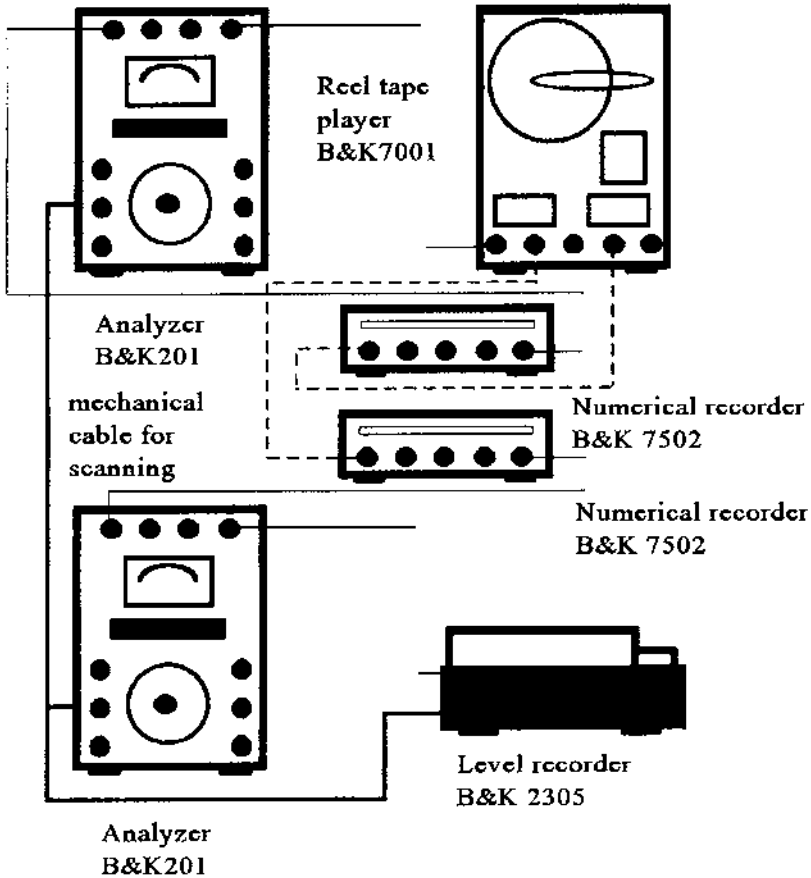


**FIGURE 2.12** Zoom analysis and Cepstrum analysis.

Initially, reference spectra and “Cepstrums” for the gearbox, accepted as functioning in good condition, have been recorded. Modifications of the spectrum on the gearing frequency and its harmonics have been observed by introducing a damaged gear wheel into the gearbox (position 4 in the kinematic schema); in addition, the global noise level increased by 3 dB. Using Cepstrum analysis, an increase of approximately three times over the reference level of the first harmonic, corresponding to the rotational frequency of the fault wheel (radial runout) was observed. Thus the advantages of Cepstrum analysis were high-

lighted, advantages related to a special sensibility and a simplification of data interpretation, because in cepstru the periodical peaks from the frequency spectrum are cumulated.

## **2.4 DIAGNOSIS OF BELT TRANSMISSIONS**

Belt transmissions generally produce a reduced noise and they even have the quality of attenuating the vibrations produced by other sources from the kinematic chains. The three main causes that lead to the occurrence of vibroacoustic phenomena in this case are: the variation of the friction forces on the relative slipping of the belt on the wheel, some aerodynamic phenomena, or imperfections on the belt joint. In order to decrease the intensity of such phenomena, the following are recommended:

- Use of plastic or rubber plated belts.

- Belt stretching has to be optimum.

- Belt pulleys have to be made from nonmetallic materials with high damping capacity.

- Use of trapezoidal belts instead of flat ones.

The damaged driving wheels produce in spectrum components to the rotation frequency and its harmonics, and damaged belts generate spectral peaks on the  $f_c = vx/L$  frequencies, where  $v$  is the speed of the belt,  $x$  is the number of belt wheels, and  $L$  is the length of the belt. The belt damage can be located with the aid of a stroboscope, fixing the image by synchronizing at the  $f_c$  frequency.

## **2.5 DIAGNOSIS OF DRIVING ELECTRICAL MOTORS**

The driving of the kinematic chains of machine tools is mainly realized by asynchrony or direct current electric motors. This section deals with driving by asynchronous triphased motors. Their functioning in a stationary regime is accompanied by phenomena that are constituted of forced vibrations and noise, influencing the elastic system of the driven kinematic chain.

### **2.5.1 Vibroacoustic Phenomena of Mechanical Nature**

These phenomena are determined by the imbalance of the rotational parts, by the dynamic efforts variable in time (raised due to an incorrect

execution and/or mounting), by the vibration of the brushes on the alternator, and so on. For example, the brush noise depends on their quality and on the quality of the sliding surfaces, on the holders' guiding way, and on the contact pressure. The noise increases at the same time as the rpm  $n$  of the rotor and as the number  $z$  of the collecting lamella increase. In spectra, the brushes' noise occurs to the  $f_1 = n * z/60$  frequency and superior harmonics.

In order to identify mechanical noise, which is always combined with magnetic noise, the motor is disconnected from the power source; the electrical components of the noise disappear immediately, allowing study of the mechanical ones. The mechanical noise can be reduced by a static and dynamic equilibration of the rotor, using the slipping bearings instead of rolling bearings by the optimization of the brushes/collector pressure [4, 11].

## 2.5.2 Vibroacoustic Phenomena of Magnetic Nature

Magnetic noise of electrical engines is due to the periodic magnetic forces from the air gap of the dynamo, the magneto-driving forces, or parasite magnetic fields. In the case of asynchronous motors, the angular frequency of the parasite magnetic fields is superimposed on the harmonics of the main field, which leads to an important increase of the magnetic noise level. The parasite alternative magnetic forces arise when the stator is not circular, the rotor has no axial symmetry, or is not centered. The notches of the rotor and stator distort the magnetic field by concentrating the lines of the flux density in the air gaps from the teeth (Fig. 2.13). Under these conditions, a complex vibration is born, whose frequency is given by the equation:

$$f_m = \omega \left[ (nR_s \pm k_e) \frac{1-s}{p} \pm k_1 \right]$$

where  $\omega$  is the frequency of the electrical network (50 Hz),  $R_s$  is the rotor notch number,  $k_e$  represents electricity coefficient (0 for static eccentricity, and 1, 2, 3 for dynamic eccentricity),  $s$  represents the slip, and  $p$  represents the number of pairs of poles,  $n = 1, 2, 3, \dots$ ,  $k_1 = 0, 2, 4, 6, \dots$

Reduction of magnetic noise can be obtained by the inclination of the rotor notches or even by using rotors with double-inclined notches, executing some symmetrical electric reeling, and by reducing the air gap. The reduction of the magnetic field intensity by decreasing the excitation

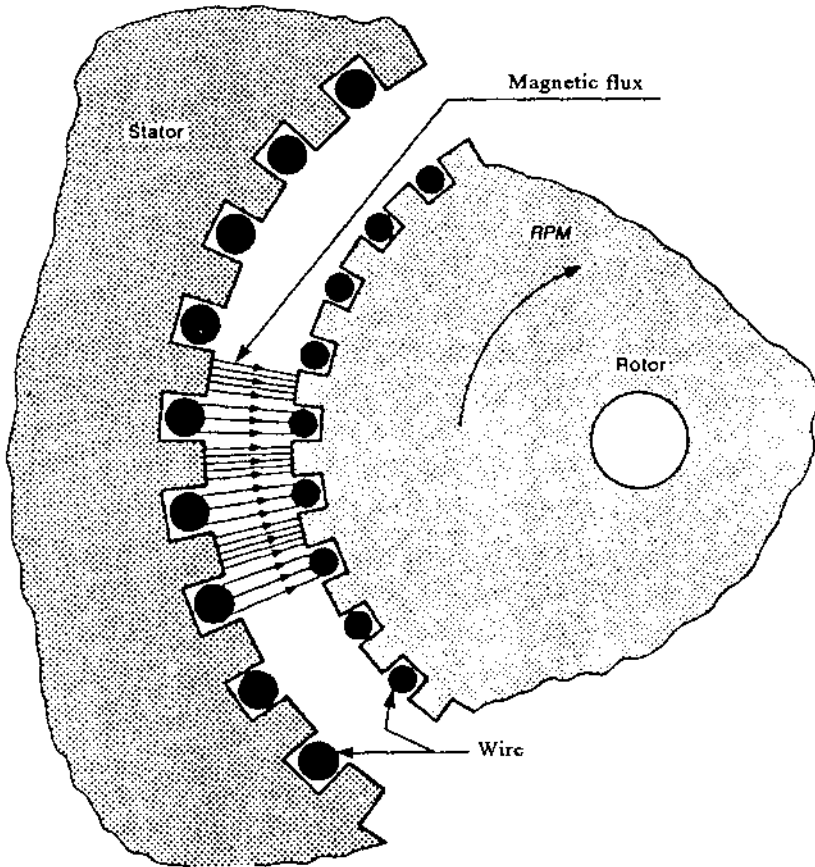


**FIGURE 2.13** Magnetic flux in an electric motor.

current leads to substantial reduction of noise; however, this measure is disadvantageous because it implies a substantial increase of motor size, for the same power.

Analysis in the frequency domain and also Cepstrum analysis allow for the detection of mechanical and magnetic damage, which occur during the functioning of the asynchronous motor. [Figure 2.14 \(left\)](#) presents a recorded example of the base spectrum (low frequency) of the functioning of a mechanical damaged motor (rupture in the motor). The effect becomes evident by the amplitude increase to the rotation frequency;

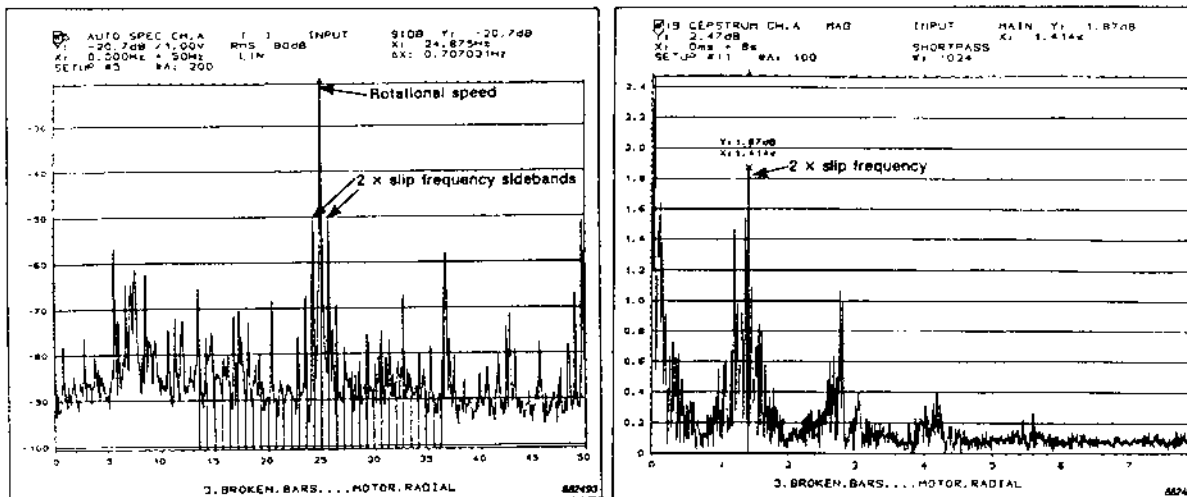


**FIGURE 2.14** Detection of mechanic and magnetic damages: (left) analysis in frequency domain; (right) Cepstrum analysis.

**TABLE 2.4** Synthesis of Direct Current and Asynchronous Motor Diagnosis Research

Vibrations cause:	Arise frequency <sup>a</sup>	Dominant plane	Observations
Lack of rotor axle poise	$1 \times f_r^a$	Radial	Unbalanced type can be established analyzing signal phase (static 0°; couple 180°; dynamic 0–180°)
Bent shaft or angular unaligned	$1 \times, 2 \times f_r$	Axial	180° axial 0° radial
Parallelism error	$1 \times, 2 \times f_r$	Radial	180° axial 180° radial
Mechanical plays	$1 \times, 2 \times, 3 \times, 4 \times f_r, \dots$ and $0.5 \times, 1.5 \times f_r, \dots$	Radial	Large number of harmonics and half harmonics
Damages of rolling bearings	Wide frequency domain (1 to 20 kHz)	—	Resonance frequencies are excited by impact with local damages from rolling paths
Incorrect lubrication (shocks) of slipping shafts	$0.43 \div 0.48 \times f_r$	Radial	Slipping bearings are used on very high power motors
Nonrigidity of stator holder, nonequilibration of phase reels' resistance, stator exfoliation	$2 \times f_R$	Radial	These damages are hard to differentiate by vibration analysis, but it is significant that they appear not only without, but also under load
Dynamical eccentricity, fissured or broken stator bars	$1 \times f_r$ and $2 \times f_a$	Radial	Bent, worn-out, or deformed rotor by local heating Slipping frequency is usually low

<sup>a</sup> $f_r$  represents the rotor rotation frequency;  $f_R$  represents the electrical network frequency;  $f_a$  represents the slipping frequency.



at the same time, lateral bands arise around this amplitude, produced by the increase of magnetic noise due to the slipping increase. Cepstrum analysis [Fig. 2.14 (right)] confirms the vibroacoustic phenomenon observed in the frequency domain.

### **2.5.3 Vibroacoustic Phenomena of Aerodynamic Nature**

The aerodynamic noise is caused by the forced circulation of the cooling air from inside the electric machine, and also by the resonance of the air from the gaps and orifices of the rotor and stator. These phenomena have a harmonic character and can be identified in the spectrum on the frequencies  $f_a = k * n * z / 60$ , where  $z$  is the number of pallets of the fan (for the noise of the air of forced cooling) or the number of rotor notches (for the rotor noise), and  $n$  is the motor rpm,  $k = 1, 2, 3, \dots$ .

Decreasing the aerodynamic resistance of the ventilation network can reduce the aerodynamic noise. Thus, aerodynamic shapes must be designed for the ventilation radial orifices of the stator and rotor; the fans must be built with aerodynamic pallets; and parts to direct the air must be designed in order to avoid the bends and narrowing of the cooling air jet. In order to avoid formation of the acoustic resonators, the existing gaps and orifices in the rotor and stator of the electric machine should be filled with phonoabsorbing material. For high rpm motors, noise attenuators for air admission and evacuation channels can be used.

Table 2.4 represents a synthesis of research in the domain of direct current and asynchronous motor diagnosis currently used in industrial drives. The superimposing of all the excitation sources presented leads to the occurrence of numerous spectral peaks. The experimental research on the vibroacoustic behavior of the usual triphase asynchronous motors (0.6 to 7.5 kW) has shown that the zone of interest of the frequency spectrum is between 16 and 530 Hz. The same domain is significant also in the case of direct current motors that are used to drive the machines and equipment.

## **2.6 DIAGNOSIS OF SOME DEVIATIONS OF THE ROTATIONAL PARTS**

The dimensional, shape, and position deviations of the motion rotational parts constitute an important source of vibrations frequently encoun-

tered on machine tools and equipment. They become more and more destructive with the increase of the machining rpm. The causes of these deviations can be execution and/or mounting errors, nonhomogeneity of the materials used (inclusions on the cast parts or density variations on the cast or forged parts), the asymmetrical configuration of some pieces, hydro- or aerodynamic phenomena, wear phenomena, and so on.

### 2.6.1 Imbalance (Lack of Poise)

Imbalance, or lack of poise, arises when the rotational and mass centers of a rotational part are not coincidental. If imbalance can be separated into a single plan, this is denominated static imbalance, and if this arises in many more planes, dynamical imbalance results.

In the case of static equilibration the two centers are made to coincide by adding or eliminating a mass on the rotational plane [the case of the grinding wheels, flying, and belt pulleys as presented in Figure 2.15 (left)]. In the case of dynamic equilibration, not only the centrifugal forces but also the coupling of these forces must be taken into consideration; this coupling produces an angular movement of the main inertial axis compared to the rotational axis. By equilibration, these two axes must be brought into coincidence [the case of rotors, Fig. 2.15 (right)]. Because of the centrifugal forces created by the unbalanced masses the following occur: dynamic forces appear in bearings formed from a primary component due to the nonequilibrated mass of the bearing plane and a secondary component due to the unbalanced coupling. The imbalance on the bearing level can be defined with the help of a turning vector whose magnitude is given by the magnitude of the resultant force

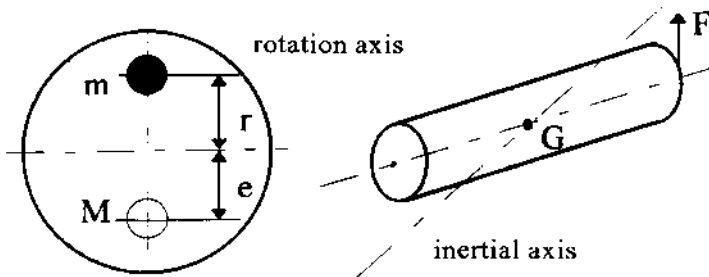


**FIGURE 2.15** Equilibration: (left) grinding wheel; (right) rotors.

and whose angle is given by its action direction. This direction may be determined precisely by comparing the phase of the signal periodically created by the vibration of the bearing with a reference periodical signal, obtained in a known position of the rotational part.

The imbalance of the rotational parts produces vibrations on the rotation frequency  $f_i = n/60$  and on the superior harmonics of this frequency, having high amplitudes especially in the radial direction. The amplitude of these vibrations increases at the same time with the increase of rpm. The imbalance also can be detected by measuring the vibration movement phase: the perturbation force is a rotational vector, so the phase will be dependent on the transducer's location, as the amplitude of the movement will practically remain constant.

### 2.6.2 Axial Imbalances

The vibrations produced by axial imbalance are characterized in the spectrum by the existence of some significant peaks of the rotational frequency and especially of its second harmonic ( $2\times$ ). The ratio between the amplitudes of the two components gives information on the degree of axial imbalance. The axial imbalance produces some high-level axial vibrations that can be perceived at both ends of the shaft with a dephasing of  $180^\circ$ , making them different from those produced by lack of poise, also located at the ends of the shaft.

### 2.6.3 Dimensional and Shape Deviations

These errors become significant on machine parts that have rolling contact (gears, bearings, ball screws, roller guidings, etc.).

In the case of gear transmission, when the leading wheel has constant angular speed, it can be observed that the angular speed of the driven wheel is influenced by the transmission errors cumulated from the dimensional and shape errors of the gear geometry. As the transmission error is a function dependent on time, each spectral component of this error will be determined by the force of interaction between the two wheels.

The shape errors of the profile ( $E_{fp}$ ) lead to an increase of up to 20 dB in the noise level of the gearing (Fig. 2.16), because their frequencies are high and can coincide with the natural transmission frequencies. These errors are signaled in the spectrum as harmonics of the gearing frequency and low harmonics of the rotation frequency [46].

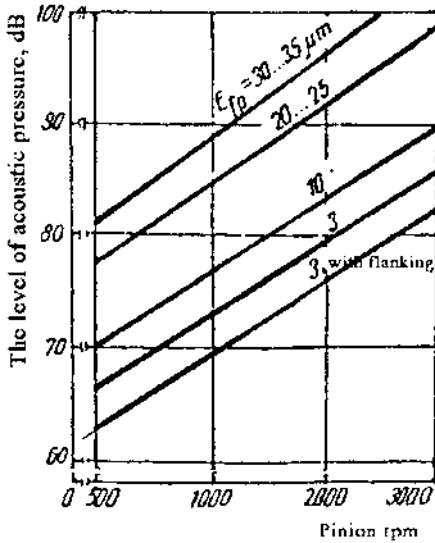


FIGURE 2.16 Noise level of gearing.

## 2.6.4 Mechanical Plays

The existence of the mechanical plays is highlighted by the presence of some strong directional vibrations, a characteristic that permits their separation from those produced by lack of poise and axial imbalance. If a harmonic load stresses an assemblage with plays, the answer of the structure is no longer harmonic, even though the frequency remains periodic (Fig. 2.17). The detection of the mechanical plays from the joints and kinematic couplings of the machine tools, even in the incipient phase, is very important because their influence on the shape and dimensional precision and quality of the part surfaces is of first rank importance.

## 2.7 DIAGNOSIS OF THE TOOL AND CUTTING PROCESS

### 2.7.1 Diagnosis of the Cutting Tool

Classifying criteria for evaluation of the integrity and wear of cutting tools have been chosen: (a) the moment of control, divided into offline

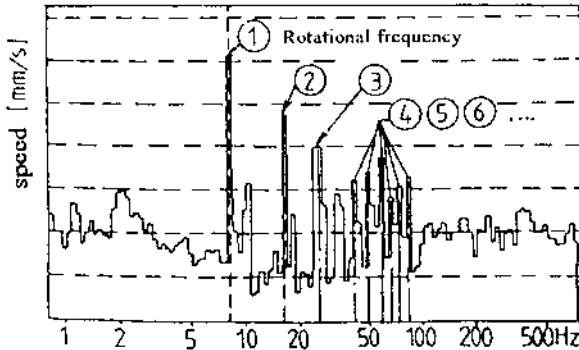


**FIGURE 2.17** Structure response when mechanical plays exist.

methods or evaluation methods outside the cutting process, and online methods or evaluation methods during the cutting process; and (b) the manner of measurement, also divided into groups: direct methods, including measurement of the cutting tool (the width of wear on the main and secondary clearance faces, the width of wear on the transversal edge, the depth of the wear crater on the rack face, and the width of the crater); and indirect methods that evaluate the wear characteristics of the tool by wear, fissuring, and breaking effects on the part or on the variation in time of some correlate measures with the cutting process.

The offline evaluation of the tool state by direct methods is usually achieved by the tool's movement in numerical command to a point whose coordinates are known, followed by the cutting edge, rack, and clearance face's palpation. The disadvantage of this method is that the tactile feelers can not perceive the integrity or the wear but only the palpation direction.

Many more direct methods without contact used to evaluate tool status exist:

- Perception of the integrity of the cutting edge (drills, taps), using pneumatic transducers [142]
- Supervising the level of radioactivity of the tool cutting edge, previously bombarded with hard particles [73]
- Wear and cracking evaluation using ultrasound sources
- Digitization of the wear surface image of the nonworn tool and its comparison, at time equal intervals, with the image of the real wear, calculating the distribution of the wear surface [97, 167]

Present online methods for evaluation of the tool state cover over 60% of total investigation techniques. They are less precise in determining the amount of wear, but they can perceive the fissure and the crack of the cutting edge and do not interrupt the manufacturing process. The most frequently used methods are discussed in the following.

### 2.7.1.1 Wear Control

Used on the basis of processing time, it considers the estimated durability of the tool.

### 2.7.1.2 Load Characteristics Evaluation of the Tool State

The Skandvik Company produces tensometric jacks that must be used in the bearing of the lead screw, because of the special sensibility of the force on the lead direction, comparative to the tool wearing. The Prometec Company, Germany, produces special bearings for the main shaft, bearings containing tensometric marks mounted in special channels of the external ring. The signal amplitude captured in this manner is proportional to the shaft load, implicit in the cutting tool. Figure 2.18 schematically presents the formation of the signal for comparison and evaluation of wear and fracture of the tool in the cylinder bore manufacturing process, using the Prometec technique (where  $P_0$  represents the

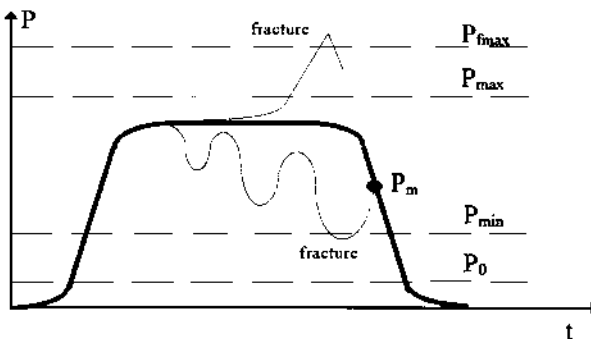


**FIGURE 2.18** Formation of the signal for comparison and evaluation of wear and fracture of the tool in the cylinder bore manufacturing process, using the Prometec technique.

minimum load level during idle run,  $P_{\min}$  represents the minimum load level during work,  $P_{\max}$  represents the reference level for the limit wear, and  $P_{f_{\max}}$  represents the reference level for the tool fracture) [23].

### 2.7.1.3 Acoustical Emission (AE) Evaluation of the Tool State

The acoustical emission signal can be correlated with specific cutting tool wear criteria. These criteria are multiple and depend on the processing type (roughing and finishing) and on the used tool. The most used criteria are wear on the clearance and/or rack face, the dimensional deviations of the part, and the roughness of the processed part.

The characteristics of the AE signal modify at the same time as the wear; an important modification of the effective value of this signal indicates the reach of the wear limit. It is interesting to note that the cutting process can be usually continued, without rupture, but in very bad conditions of geometrical shape and quality of the surface.

During the cutting process, the effective value of the AE signal has a specific evolution: progressive increase, followed by a substantial increase in the vicinity of the catastrophic wear phase (this is much more evident on tools equipped with metallic carbide plates), then an accentuated decrease until the moment of the cutting edge destruction. The same behavior is found both in the roughness and finishing cases.

Figure 2.19 presents a recording of the effective value of the acoustic emission signal on a milling machine with a mill having a single tooth, in three successive passes. The passes are separated by two zones of absence of the AE signal; during the third pass the tooth has broken, a fact highlighted by a peak, and then an abrupt decrease of the effective value of the signal.

Concerning the break of the cutting tool, the most frequent causes are the mechanical shock when meeting some hard inclusions in the material to be processed or successive mechanical shocks (on the turning of some polygonal and grooved parts), or the thermal shock as a result of interruption of the cooling liquid. Tool break is easily highlighted by supervising the effective value of the AE signal because of the transitory energy jump. A typical example of tool breaking, hard to highlight by other methods, is the breaking of the auger when boring (Fig. 2.20). The tool-part contact is well detected by supervising the effective value of the AE signal and is clearly separated from the breaking zone (between the dashed lines) and from the zone of ulterior rack of the tool.

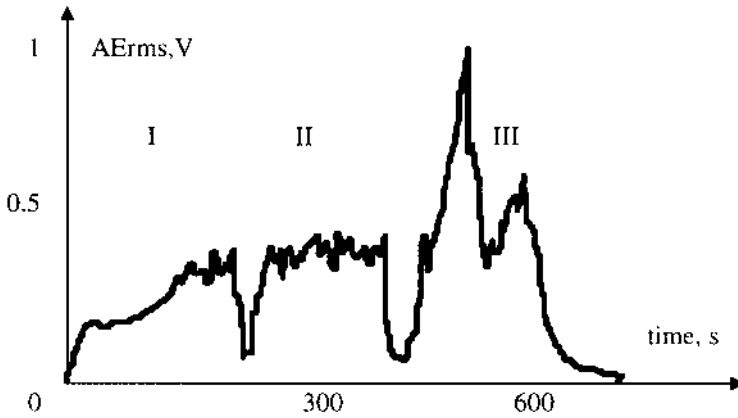


**FIGURE 2.19** Recording of the effective value of the acoustic emission signal on a milling machine with a mill having a single tooth, in three successive passes.

In conclusion, the AE method is applicable and already widely used for the detection of tool breakage, but monitoring tool wear in the same manner is a more complicated problem because of many factors. Finding the wear criterion that best correlates with the evolution and the value of some specific dimensions of the AE signal for roughing and

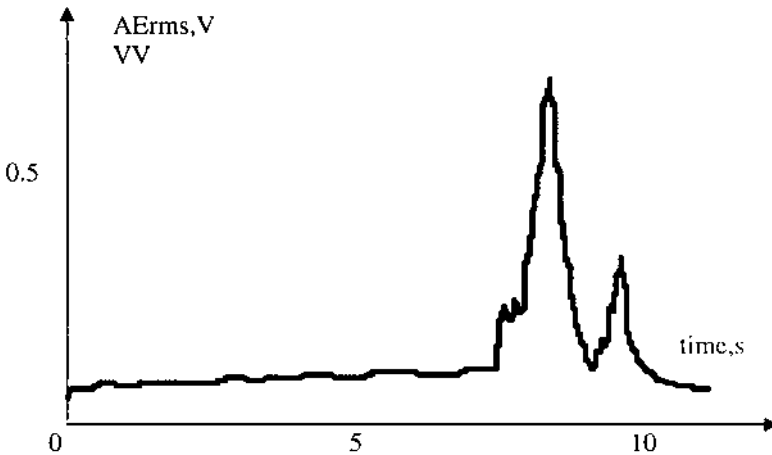


**FIGURE 2.20** A typical example of tool breaking.



finishing operations in the case of different cutting processes remains another experimental study problem and requires the accumulation of an important database.

#### **2.7.1.4 Electrical Resistance Monitoring**

This monitors the tool-part contact or the thermoelectromotoric tension that arises during processing. The contact resistance in the tool-part zone is of  $10^{-4}$  to  $10^{-2}$   $\Omega$  compared to  $10^2$  to  $10^3$   $\Omega$ , the resistance of the bearings and  $10$  to  $10^2$   $\Omega$ , the electrical resistance due to the cooling-lubricating fluid. The fissure or fracture of the cutting edge produces an increase of up to 30% and then an abrupt decrease to zero of the voltage in the measuring circuit [122].

H. Wiele and P. Metz [165] highlighted the possibility of supervising tool wear by estimating the thermal gradient. Placing two thermocouples under the cutting plate, they discovered that the difference between the contraelectromotor voltages of the two controlled points is proportional to the wear on the clearance face. The disadvantages of these two methods consist of the difficult emplacement of the transducers, and also on the sensibility of the thermoelectromotor voltage on the variations of the tool geometry and of the parameters of the cutting regime.

Recently, Romanian researchers have grappled with the domain of diagnosis of the cutting tool state in their doctoral theses. E. Carata [23] brought important contributions on the elaboration of a research methodology in order to determine online the tool wear on boring, by vibroacoustic methods. L. Bogdan [12] correlated the information on three parameters (noise, vibration, and temperature) in order to evaluate the state of the cutting tool.

#### **2.7.2 Diagnosis of the Cutting Process**

The cutting process generates elastic waves that transmit to the working piece and the tool and its support. An acoustical emission transducer, placed in the vicinity of the cutting zone, can detect them, and the perceived signal is a “signature” characteristic of the cutting conditions.

At the beginning of the 1990s, T. Moriwaki [110, 111] proposed a supervising scheme of the acoustical signal in cutting, which today is widely accepted (Fig. 2.21). The inferior cutting frequency of the filter set used is 100 kHz, in order to avoid the vibroacoustic signals associated with the system machine tool-clamping device-tool-part. The superior cutting frequency is 10 Mhz, in order to avoid electrical noise; the

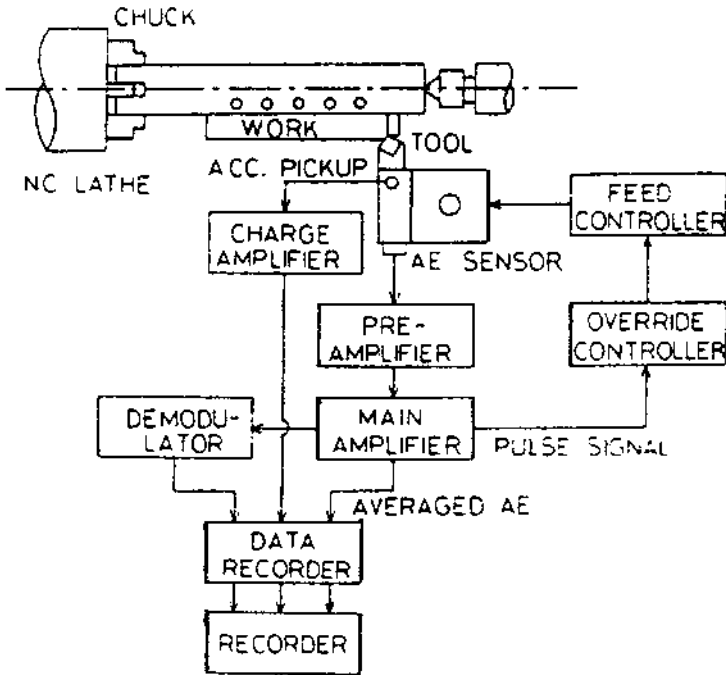


**FIGURE 2.21** Supervising scheme of the acoustical signal in cutting.

natural nominal frequency of the transducer of acoustical emission can be approximately 500 kHz. This scheme has provided an identification method for acoustical emission sources specific to the cutting process; in addition, this scheme allows the determination of the characteristic frequencies and the realization of a correlation between the development of the cutting process and magnitudes characteristic of the acoustical emission signal.

The main sources of acoustical emission in the cutting process are (according to Souquet, Weber, and Dornfeld; Fig. 2.22):

- Plastic deformation in the shearing zone
- Friction of the chip on the rack face of the cutting tool
- Cutting edge deposits
- Friction between tool and processing part
- Collision and friction between chip and part
- Fragmentation of the chip
- Friction of the chip on the chip breaker [70, 84, 107]

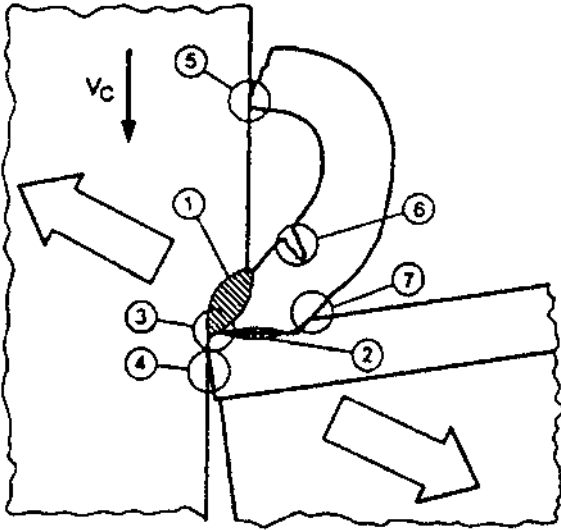


**FIGURE 2.22** Main sources of acoustical emission in the cutting process.

The analysis of the signals of these sources provided data for a mathematical model that connected the effective value of the AE signal ( $AE_{RMS}$ ) with the parameters of the cutting regime (cutting speed, cutting depth). Experimental research on turning and boring has confirmed the validity of the model for orthogonal cutting. In the milling case, difficulties occur because of the presence of shocks when each tooth touches the part.

The proposed mathematical model has proved efficient both for supervising the evolution of the cutting tool wear and to detect its breakage, especially where the cutting conditions do not allow visualization of the tool (boring):

$$AE_{RMS} = C \sin \alpha \left[ \tau_k b_l V \left( \frac{t_l \cos \alpha}{\sin \phi \cos(\phi \alpha)} + \frac{1}{3} (1 + 2t_l) \frac{\sin \phi}{\cos(\phi \alpha)} \right) \right]^{1/2}$$

where  $C$  is an experimental constant,  $\alpha$  is the tool's attack angle,  $\phi$  is the cutting angle,  $\tau_k$  is the cutting stress,  $b_l$  is the cutting length,  $l_l$  is the chip-tool contact length,  $t_l$  is the thickness of the uncut chip, and  $V$  is the tangential cutting speed.

The acoustical emission signal ( $AE_{RMS}$ ), converted in the frequency domain, can look different depending upon the emplacement

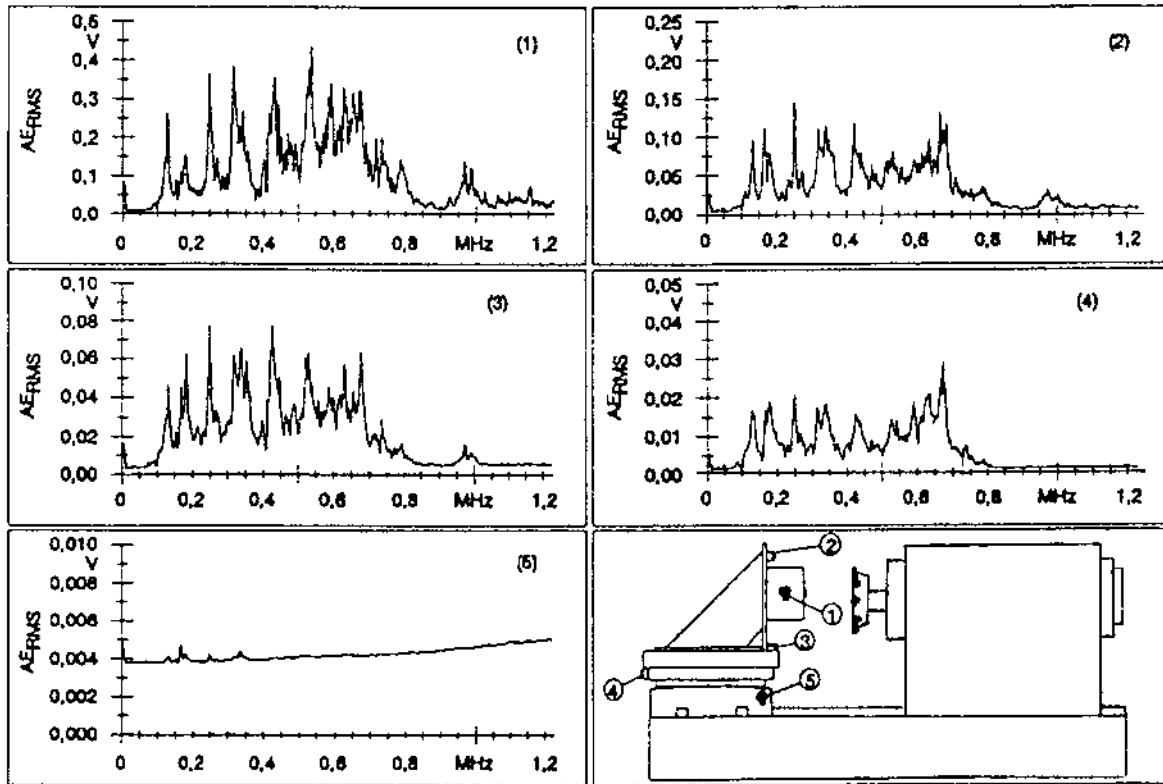
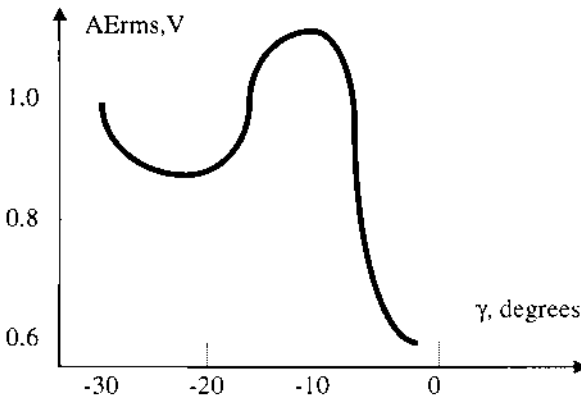


FIGURE 2.23 Acoustical emission signal ( $AE_{RMS}$ ), converted in the frequency domain.

of the transducer, as shown in [Figure 2.23](#). The most advantageous positions for emplacement are directly on the part (1) or on the part clamping device (3,2).

Supervising the acoustical emission has imposed the grouping of the influence factors into three categories: parameters bound to the nature of the processed material (hardness, the capacity of being processed); parameters connected to the material and geometry of the cutting tool; and parameters of the working regime (the speed and depth of cut and feed). Concerning the factors from the first category, it has been observed that the level of acoustical emission varies proportionally with the material hardness, and the differences of the capacity of being processed modify only slightly the characteristics of the AE signal. For example, for an increase of hardness with 300 Brinell units, the level of acoustical emission can increase by approximately 15 dB. As to the factors in the second category, the estimation is that not the nature of the tool material but the way that materials are preponderantly degrading (abrasion, fissure, chemical diffusion) affects the acoustical emission signal. The modification of the cutting tool geometry has a significant effect on the energy of the acoustical emission signal. From this point of view, the most important parameter is the rack angle; experimental research (Kannatey-Asibu and Dornfeld) has shown that the medium of the acoustical emission signal energy sensibly modifies on the increase of the rack angle ([Fig. 2.24](#)). One of the effects of the rack angle increase



**FIGURE 2.24** Medium of the acoustical emission signal energy depending on the rack angle.

is the increase of the contact length chip-tool; consequently, a similar dependency will be observed also between this rack angle and the energy of the acoustical emission signal. Systematic tests (Moriwaki, Souquet, Deschamps, Weber, Herberger, Diei, and Dornfeld) concerning the influence of the cutting regime parameters on the acoustical emission level have shown that the effective value of the acoustical emission signal is proportional to the square of the cutting speed (Fig. 2.25a) and also to the square of the depth of cut (Fig. 2.25b). The influence of the feed magnitude on the AE signal is negligible [32, 33]. During experimental research, it has been noticed that the use of cooling-lubricating liquids decreases the effective value (RMS) of the acoustical emission signal.

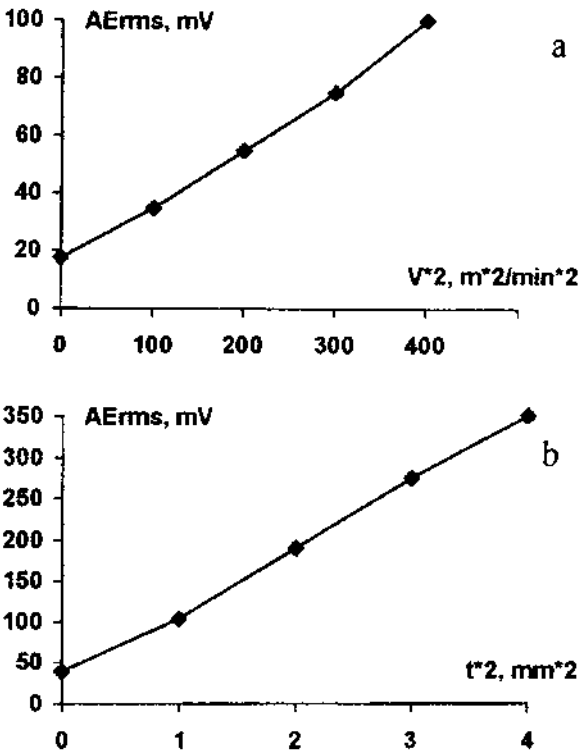


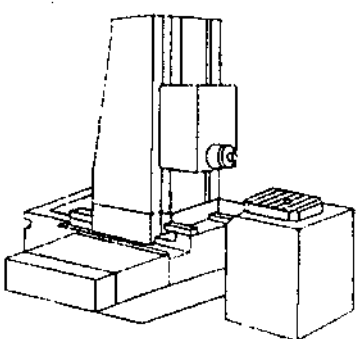
**FIGURE 2.25** Influence of cutting regime parameters on acoustical emission level; acoustical emission signal is proportional to: (a) the square of the cutting speed; (b) the square of the depth of cut.

## 2.8 TECHNICAL DIAGNOSIS IN FLEXIBLE PROCESSING SYSTEMS

Modern machine tools are integrated in flexible production systems that include parts and/or tool feeding systems, parts and/or tool store systems, numerical or computer-assisted control systems, systems of adaptive or optimal control, and so on, and each component of the system develops specific actions. From this point of view, a matrix representation of the production system (Fig. 2.26) leads to a better understanding of its problems; one of these problems may be, for example, the prediction and diagnosis of the machine tool and/or cutting tools destined to fail [145, 35].

The normal functioning state of the flexible cutting systems supposes the optimal and simultaneous accomplishment of many fundamental functions:

- Automatic processing
- Automation of the flows (materials, tools, parts)
- Control, supervisory, diagnostic, and automatic maintenance
- Informational integration

ACTION \ OBJECT	Detection of failures (alarming)	Tools control (CNC)	Prediction and diagnosis of faults	Adaptive control ACT - ACG
Machine-tool (including tool magazine and pallets)				
Tools - wear supervising; - detection of rupture.				
Cutting process (auto-vibrations and forced vibrations control)				
Numerical command (CNC - DNC)				

**FIGURE 2.26** Matrix representation of a production system.

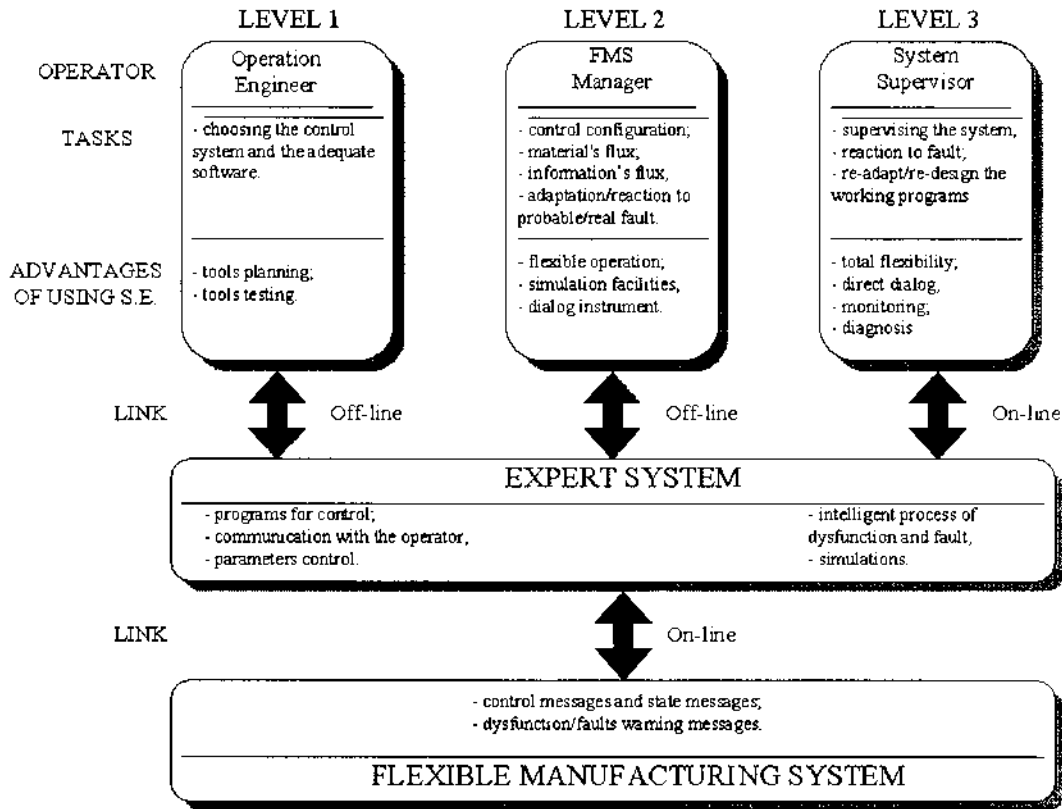


**FIGURE 2.27** Expert system for the direction of flexible manufacturing systems.



The laboratory of Machine Tools of the University of Aachen has devised an expert system for the direction of flexible manufacturing systems [163, 83]. In its frame, the diagnostic function appears on the most complex level, and the monitoring has a permanent character (Fig. 2.27).

Accomplishing the diagnostic function involves a rapid and correct evaluation of the damage messages and deduction of the reasons for these damages, possible or existent. In this respect, an important amount of information is processed, considering that damage may also have many different causes. A correct diagnosis most often requires an oriented request of supplementary information; statistical and heuristic data are requested and the system must have the capacity to adapt to the new experiments and accumulations. This is not possible using conventional programming methods because the combinations (message of damage, the cause) are practically infinite; that is why the expert system does not describe the problems as sequential algorithms, but as relations and functional dependencies.

The presented expert system also has the capacity to recommend and even to execute a series of corrective actions as a result of establishing the technical diagnosis. The reaction time is very short, the information processing usually being done in real-time.

## **2.9 CONCLUSIONS: THEORETICAL AND EXPERIMENTAL RESEARCH PERSPECTIVES**

Supervision of the functional state of machine tools and of the manufacturing processes developed by them have become subjects of wide interest in the last decade. The most important reasons for this phenomenon are:

Unexpected stops of machines produce significant financial loss to companies, especially in those plants that use optimized plans for their production.

Monitoring and diagnosis lead to the increase of the machines' autonomy, allowing their intensive use in two or three shifts.

Monitoring and diagnosis lead to increases in productivity and production quality.

The cost of installation and maintenance of the monitoring and diagnostic systems is decreasing continuously, and at the same time the cost of the machine tools is increasing because of the increase of their complexity.

By analysis of some technical parameters that correlate with the functional state of the machine tool (mechanical vibrations, noise and acoustical emission, temperature, force, cutting moment, etc.), a series of monitoring and diagnosis methods has been identified. Two classification systems of diagnosis exist: diagnosis methods of surface, which indicate only the functioning state and/or the existence of damage; and diagnosis methods of profoundness, which allow for the appreciation of the nature, location of damage, and time until the machine stops.

Not all acquisitioned signals from the functioning machine tool contain useful diagnostic information. An example of this is the forced vibrations coming from a discontinuous cutting process, vibrations that provoke fluctuations of the cutting forces, and the mechanical resonance of the machine. Another example is the trepidation phenomenon (chatter) that induces vibrations in the entire machine level. Both examples present structural vibrations but they are regarded as major damage by an inadequate monitoring and diagnosis system.

The literature has shown that relevant research exists concerning diagnosis of some elements of machine tool structure which are common to other types of machines and equipment (bearings, gearing, and belt transmissions). The diagnosis of cutting tools and the cutting process is an intensively investigated domain. The methods used in diagnosis are very diverse, and dependent upon the university or researcher who investigates them; often they do not have a systemic character or can not be reproduced. Considering these aspects, this research endorses the systemic approach of the diagnostic methods useful in the machine tool domain and their application on the kinematic chain level, especially for the feed kinematic chain, where the diagnostic information is missing. This work proposes the theoretical and experimental verification of the physical model of the investigated feed kinematic chain, in order to remove the possibilities of false diagnostics provoked by an inadequate structural behavior.

Theoretical and experimental research should be oriented to the determination by calculation of the characteristic frequencies of the functioning of the specific feed kinematic chains (bearings, ball screws, roll cam follower, lug) because of their role in identifying mechanical damage.

Cognizant of the recent performance of computing systems, this work proposes the introduction of virtual instrumentation in the vibroacoustic diagnosis of machine tools, by elaborating and providing users with virtual diagnosis apparatus that has increased performance capacity compared with traditional investigation equipment.

Last but not least, the role of this work is to create a databank based on the findings of technical diagnosis by vibroacoustic methods so that further developments of machine tool diagnosis on the level of expert systems can be realized.